Transactions on Machine Intelligence 1(2) (2018) 57–69

ISSN Online: 2821-1693

Transactions on Machine Intelligence

Journal Homepage: https://tmachineintelligence.ir/index.php/TMI

Design of a Terminal Sliding Mode Controller for Distributed Generation Systems Based on Multi-Agent Systems

M. Mazaheri[1], R. Ghasemi[2,*]

[1] Master's Student, Electrical Engineering, University of Qom, Qom, Iran
[2] Associate Professor, Electrical Engineering, University of Qom, Qom, Iran

ARTICLE INFO

Article History:
Received 4 March 2018
Received in revised form 15 May 2018
Accepted 8 June 2018
Available online 27 June 2018

Keywords:
Multi-Agent Systems, Distributed Generation, Smart Grid, Terminal Sliding Mode Control, Wind Turbine, Photovoltaic

ABSTRACT

Distributed generation is a new trend in electric power production. These units are placed in substations and distribution feeders near loads, and are used either independently or in parallel with electrical grids. The use of "intelligent agents" refers to agents that must operate robustly in open, unpredictable environments where significant changes may occur. In this paper, wind turbines and photovoltaic systems are considered as distributed generation agents, with each of these elements treated as an individual agent. Given the heterogeneity of these agents, the system is considered heterogeneous, complicating problem-solving. To address this issue and convert it into a homogeneous problem, it is assumed that identical agents have separate leaders, and if all agents are synchronized, the heterogeneous problem can be effectively treated as a homogeneous one. Following the leader is achieved using a terminal sliding mode controller, with the primary advantages of this method being overall system stability, finite-time convergence, and agent synchronization.

1. INTRODUCTION

The power grid is evolving towards what is known as "smart grids." The development of communication infrastructures and power electronics interfaces with control capabilities enables the management of complex systems in efficient and scalable ways. Multi-Agent Systems (MAS) based on the distribution of information and computational algorithms provide an excellent technological solution for these applications. This research focuses on the applications of MAS in power systems, demonstrating how they can be integrated with other artificial intelligence techniques to create a smarter and more flexible grid.

Implementing a control network based on multi-agent systems (MAS) capable of making intelligent decisions on behalf of the user has become the focus of extensive research in this field [1]. Frequency control of an isolated microgrid is achieved through the management of energy storage, such as superconducting magnetic energy storage and battery energy storage, as well as the control of existing distributed generators, including wind turbines, microturbines, and load control capabilities. Frequency control in an isolated microgrid is more challenging than in conventional power systems [2,3]. Expert systems can contribute to the instantaneous power injection for primary

* Corresponding Author: R.ghasemi@qom.ac.ir
Associate Professor, Electrical Engineering, University of Qom, Qom, Iran

http://dx.doi.org/10.47176/TMI.2018.57

frequency control [4]. Consequently, the appropriate distribution of distributed generators (DGs) is recognized as playing a significant role in the stability and frequency regulation of a microgrid under new equilibrium conditions [5,6]. A hierarchical frequency control scheme for centralized microgrid control to achieve improved frequency coordination between expert systems and DGs is presented in [7,8]. Moreover, the corresponding hierarchical frequency control and multi-agent systems require a powerful Microgrid Central Controller (MGCC) [9, 11], which is expensive and susceptible to failures when handling a vast amount of data. In [11], a stable load shedding (LS) algorithm based on multi-agent systems for power systems is proposed and emphasized. A MAS-based scheme for a microgrid is presented in [12].

An agent can perceive its environment and make decisions in response to environmental changes, independently resolving issues according to its objectives [13, 14]. Given that the characteristics of multi-agent systems are well-suited for the operation of microgrids, it has been demonstrated that agent-based operations are efficient for microgrid management and also for smart grid operations. Research has focused on the operation of microgrids using multi-agent systems [15]. In the proposed system, agents collect information from each component and send it to the decision-making agent.

In this paper, wind turbines and photovoltaic systems are considered as distributed generation agents, with each of these elements treated as an individual agent. Due to the differences among the agents, the system is considered heterogeneous, which complicates problem-solving. To address this issue and convert it into a homogeneous problem, it is assumed that identical agents have separate leaders. If all agents are synchronized, the heterogeneous problem can effectively be treated as a homogeneous one. Leader-following is achieved using terminal sliding mode control, and the main advantages of this method are overall system stability, finite-time convergence, and agent synchronization.

The dynamic equations of wind turbines and photovoltaic systems are discussed in Section 2. Section 3 focuses on the design of the multi-agent sliding mode controller, and the simulation results are examined in Section 4. Finally, the paper concludes with the conclusion section.

2. DYNAMIC EQUATIONS OF WIND TURBINE AND PHOTOVOLTAIC

This section presents the dynamic models of wind turbines and photovoltaic systems. In the equations describing the wind turbine, the stator and rotor currents are considered as outputs, and the stator and rotor voltages are considered as inputs. The equations can be expressed as follows.

$$v_{ds} = -R_s i_{ds} - \omega_s \psi_{qs} + \frac{d\psi_{ds}}{dt} \tag{1}$$

$$v_{qs} = -R_s i_{qs} + \omega_s \psi_{ds} + \frac{d\psi_{qs}}{dt} \tag{2}$$

$$v_{dr} = -R_r i_{dr} - s\omega_s \psi_{qr} + \frac{d\psi_{dr}}{dt} \tag{3}$$

$$v_{qr} = -R_r i_{qr} + s\omega_s \psi_{dr} + \frac{d\psi_{qr}}{dt} \tag{4}$$

Where v denotes voltage, R denotes resistance, i denotes current, ω_s denotes the electrical frequency of the stator, ψ denotes the flux linkage, and s denotes rotor slip. Moreover, d and q specify the direct and quadrature axis components, respectively.

$$\psi_{ds} = -(L_s + L_m) i_{ds} - L_m i_{dr} \tag{5}$$

$$\psi_{qs} = -(L_s + L_m) i_{qs} - L_m i_{qr} \tag{6}$$

$$\psi_{dr} = -(L_r + L_m)i_{dr} - L_m i_{ds} \tag{7}$$

$$\psi_{qr} = -(L_r + L_m)i_{qr} - L_m i_{qs} \tag{8}$$

The mutual inductance is denoted by Lm, while the self-inductances of the stator and rotor are denoted by Ls and Lr respectively. The rotor slip s is defined as follows:

$$s = \frac{\omega_s - \frac{p}{2}\omega_m}{\omega_s} \tag{9}$$

where p is the number of poles, and ω_m is the mechanical frequency of the generator. The active and reactive power generated by the wind turbine are given as follows:

$$P = v_{ds}i_{ds} + v_{qs}i_{qs} + v_{dr}i_{dr} + v_{qr}i_{qr} \tag{10}$$

$$Q = v_{qs}i_{ds} - v_{ds}i_{qs} + v_{qr}i_{dr} - v_{dr}i_{qr} \tag{11}$$

Now we can express the above equations in the following state-space form.

$$x = [i_{ds}\ i_{qs}\ i_{dr}\ i_{qr}]^T \tag{12}$$

$$U = [v_{ds}\ v_{qs}\ v_{dr}\ v_{qr}]^T \tag{13}$$

$$y = Ix \tag{14}$$

$$A_1\dot{x} + A_2 x = Iu \tag{15}$$

In the above equation, the model parameters can be expressed as follows:

$$A_1 = \begin{bmatrix} -(L_s + L_m) & 0 & -L_m & 0 \\ 0 & -(L_s + L_m) & 0 & -L_m \\ -L_m & 0 & -(L_r + L_m) & 0 \\ 0 & -L_m & 0 & -(L_r + L_m) \end{bmatrix} \tag{16}$$

$$A_2 = \begin{bmatrix} -R_s & \omega_s(L_s + L_m) & 0 & \omega_s L_m \\ -\omega_s(L_s + L_m) & -R_s & -\omega_s L_m & 0 \\ 0 & s\omega_s L_m & -R_r & s\omega_s(L_r + L_m) \\ -s\omega_s L_m & 0 & -s\omega_s(L_r + L_m) & -R_r \end{bmatrix} \tag{17}$$

$$I = \begin{bmatrix} 1 & 0 & 0 & 0 \\ 0 & 1 & 0 & 0 \\ 0 & 0 & 1 & 0 \\ 0 & 0 & 0 & 1 \end{bmatrix} \tag{18}$$

Now, after multiplying the equation by the inverse of A_1, the state-space representation can be expressed as follows.

$$\dot{x} = -A_1^{-1}A_2 x + A_1^{-1}u \tag{19}$$

$$A = -A_1^{-1}A_2 \quad . \quad H = A_1^{-1} \tag{20}$$

$$\dot{x} = Ax + Hu \tag{21}$$

$$y = Ix \tag{22}$$

In this section, the dynamics of the photovoltaic system are introduced. The dynamic model of the grid-connected solar cell system, in which the DC voltage produced is converted to three-phase voltage by an inverter and an LCL filter, is presented.

Now, using the Park transformation (abc/dq), we can transform the three-phase output voltage of the inverter into dq coordinates. Consequently, the equations for the current and output voltage of the inverter in dq coordinates are written as follows.

$$i'_{2d} = \frac{v_{cd}}{L_2} + \omega i_{2q} - \frac{1}{L_2} v_{gd} \tag{23}$$

$$i'_{2q} = \frac{v_{cq}}{L_2} - \omega i_{2d} - \frac{1}{L_2} v_{gq} \tag{24}$$

$$\dot{v}_{cd} = \frac{i_{1d}}{C_f} + \omega v_{cq} - \frac{1}{C_f} i_{2d} \tag{25}$$

$$\dot{v}_{cq} = \frac{i_{1q}}{C_f} - \omega v_{cd} - \frac{1}{C_f} i_{2q} \tag{26}$$

$$i'_{1d} = \frac{v_d}{L_1} + \omega i_{1q} - \frac{1}{L_1} v_{cd} \tag{27}$$

$$i'_{1q} = \frac{v_q}{L_1} - \omega i_{1d} - \frac{1}{L_1} v_{cq} \tag{28}$$

Now, the state variable for the photovoltaic cell is defined as $x = [i_{2d}\ i_{2q}\ v_{cd}\ v_{cq}\ i_{1d}\ i_{1q}]^T$, and the control input is defined as $U = [v_{gd}\ v_{gq}\ v_d\ v_q]^T$. The output is also considered as y = x. The state-space representation can be expressed as follows.

$$\dot{x} = Ax + Hu \tag{29}$$

$$y = Ix \tag{30}$$

In the above relationship, the coefficients and matrices can be expressed as follows.

$$A = \begin{bmatrix} 0 & \omega & \frac{1}{L_2} & 0 & 0 & 0 \\ -\omega & 0 & 0 & \frac{1}{L_2} & 0 & 0 \\ -\frac{1}{C_f} & 0 & 0 & \omega & \frac{1}{C_f} & 0 \\ 0 & -\frac{1}{C_f} & -\omega & 0 & 0 & \frac{1}{C_f} \\ 0 & 0 & -\frac{1}{L_1} & 0 & 0 & \omega \\ 0 & 0 & 0 & -\frac{1}{L_1} & -\omega & 0 \end{bmatrix} \tag{31}$$

$$H = \begin{bmatrix} -\frac{1}{L_2} & 0 & 0 & 0 \\ 0 & -\frac{1}{L_2} & 0 & 0 \\ 0 & 0 & 0 & 0 \\ 0 & 0 & \frac{1}{L_1} & 0 \\ 0 & 0 & 0 & \frac{1}{L_1} \end{bmatrix} \tag{32}$$

The objective is to unify the d and q components of the filter output current for all photovoltaic cells. These components are our outputs. If we use the Park transformation (dq/abc) to convert the d and q components to three-phase, and assuming the d and q components of the filter output current are unified for all photovoltaic cells, then the amplitude and frequency of the three-phase output current will be identical for all cells. To achieve this goal, we must write the consensus error for the output and aim to minimize this error towards zero. If this error approaches zero, then the d and q components of the filter output current will be identical for all photovoltaic cells.

Considering that sunlight is uncertain and not always available, the output current also has uncertainty. We assume that the d component of the input current, the capacitor voltage, and the output current have disturbances. Additionally, we assume there are M photovoltaic cells. The state-space equations for the j -th photovoltaic cell are written as follows. $X_j = [X_{j.1} \quad \dots \quad X_{j.M}]$ is the state variable, U_j is the input, Y_j is the output, and Dj is the disturbance corresponding to the j-th cell.

$$\dot{X}_j = AX_j + HU_j + RD_j \tag{33}$$

$$Y_j = IX_j \tag{34}$$

$$R = \begin{bmatrix} 1 & 0 & 0 \\ 0 & 0 & 0 \\ 0 & 1 & 0 \\ 0 & 0 & 0 \\ 0 & 0 & 1 \\ 0 & 0 & 0 \end{bmatrix} \tag{35}$$

Now, considering the dynamic equations of each photovoltaic element and turbine, in the next section, we will proceed with the design of a sliding mode controller for the multi-agent system.

3. DESIGN OF SLIDING MODE CONTROLLER FOR MULTI-AGENT SYSTEM

In the context of designing a multi-agent sliding mode controller, consider the following dynamic equations of a single agent:

$$\dot{X}_j = AX_j + HU_j + RD_j \tag{36}$$

$$Y_j = IX_j \tag{37}$$

$$R = \begin{bmatrix} 1 & 0 & 0 \\ 0 & 0 & 0 \\ 0 & 1 & 0 \\ 0 & 0 & 0 \\ 0 & 0 & 1 \\ 0 & 0 & 0 \end{bmatrix} \tag{38}$$

Given that $X_j = [X_{j.1} \quad \dots \quad X_{j.6}]^T$ is the state variable, Uj is the input, Yj is the output, and Dj is the disturbance corresponding to the j -th cell, we now consider a multi-agent system composed of several photovoltaic cells. These cells influence each other, and the effects of the currents from other photovoltaic cells on each other can be represented using the adjacency matrix A_{adj} in the overall system dynamics.

To achieve this, we express the system using the Kronecker product as follows:

Assuming $X = [X_1 \quad \dots \quad X_N]^T$ ، $U = [U_1 \quad \dots \quad U_N]^T$ ، $D = [D_1 \quad \dots \quad D_N]^T$ and $Y = [Y_1 \quad \dots \quad Y_N]^T$ the relationship can be rewritten as follows:

$$\dot{X} = (I_N \otimes A)X + (I_N \otimes R)D + (I_N \otimes H)U \tag{39}$$

Additionally, the dynamics of the leader can be expressed as follows:

$$\dot{X}_0 = (I_N \otimes A)X_0 + (I_N \otimes H)r \tag{40}$$

Now, we need to write the consensus error for the output Y_i.

$$e_i = -\sum_{j=1, j\neq i}^{N} a_{ij}\left(Y_i - Y_j\right) - b_i(Y_i - Y_0) \tag{41}$$

In the above relationship, $Y_0 = [1 \dots 1]^T$ holds. Furthermore, according to the properties of the Kronecker product, the above relationship can be expressed as follows:

$$E = -([L + B] \otimes I_4)Y + (B \otimes I_n)Y_0 \tag{42}$$

In this relationship, L is the Laplacian matrix of the graph. Considering the properties of the Laplacian matrix, the above relationship can be expressed as follows:

$$E = -([L + B] \otimes I_n)(Y - Y_0) \tag{43}$$

Now, by taking the derivative, the consensus error dynamics are obtained as follows:

$$\dot{E} = -([L + B] \otimes I_n)(\dot{Y} - \dot{Y}_0) \tag{44}$$

Given $\dot{Y}_i = I\dot{X}_i$ and $\dot{Y}_0 = I\dot{X}_0$, the following relationship can be obtained:

$$\dot{E} = -([L + B] \otimes I_n)\{(I_N \otimes A)X + (I_N \otimes R)D + (I_N \otimes H)U - (I_N \otimes A)X_0 - (I_N \otimes H)r\} \tag{45}$$

Considering the property of the Kronecker product, we have:

$$(I_n \otimes A).(B \otimes I_m) = (I_n.B) \otimes (A.I_m) = (B.I_n) \otimes (I_m.A) = (B \otimes I_m).(I_n \otimes A) \tag{46}$$

As a result, the consensus error dynamics can be expressed using the property of the Kronecker product as follows:

$$\dot{E} = -([L + B] \otimes I_n)(I_N \otimes A)(X - X_0) - ([L + B] \otimes I_n)(I_N \otimes R)D - ([L + B] \otimes I_n)(I_N \otimes H)(U - r) \tag{47}$$

Now, considering the relationships $Y = I_N X$ and $\mathrm{E} = -([L + B] \otimes I_{\mathrm{n}})(Y - Y_0)$, the consensus error dynamics are derived as follows:

$$\dot{E} = \underbrace{([L + B] \otimes I_n)(I_N \otimes A)([L + B] \otimes I_n)^{-1}}_{\acute{A}} E - \underbrace{([L + B] \otimes I_n)(I_N \otimes R)}_{\acute{R}} D - \underbrace{([L + B] \otimes I_n)(I_N \otimes H)}_{\acute{H}} (U - r) \tag{48}$$

In the process of designing a sliding mode controller, the sliding surface is considered as $S = \lambda^T E$, where λ is a vector of appropriate dimensions. The sliding surface dynamics are obtained as:

$$\dot{S} = \lambda^T \dot{E} = \lambda^T \left(\acute{A}E - \acute{R}D - \acute{H}(U - r) \right) \tag{49}$$

Now, let us consider the Lyapunov function as $V = \frac{1}{2} S^2$. The derivative of the Lyapunov function is given by:

$$\dot{V} = S\dot{S} = S\left\{ \lambda^T \left(\acute{A}E - \acute{R}D - \acute{H}(U - r) \right) \right\} \tag{50}$$

For the system to be stable, the derivative of the Lyapunov function must be negative definite:

$$\dot{V} = S\dot{S} \leq -\eta |S| \tag{51}$$

The control input is considered as $U = U_r + U_{eq}$, where U_{eq} is designed to eliminate the deterministic terms of the system and Ur *to* counteract the system disturbances. Thus, we have:

$$U_{eq} = r + \acute{H}^{-1} \acute{A}E - \acute{H}^{-1} \acute{R}D \tag{52}$$

$$U_r = -ksign(S) \tag{53}$$

Considering the magnitude of disturbances, the maximum gain can be determined as:

$$D = [d_i] \longrightarrow |d_i| \leq d_{i.Max} \longrightarrow D_{Max} = [d_{i.Max}] \tag{54}$$

The proposed method in this section will be implemented on photovoltaic and wind turbine systems.

4. SIMULATION RESULTS

Let us consider a system equipped with three solar cells and three wind turbines. The objective is to synchronize and equalize the d and q components of the currents of both the wind turbines and the solar cells.

4.1. Simulation and Results of the Designed Controller for Wind Turbines

By applying the controllers designed in the previous section, the simulation results are as follows.

The parameter values of the wind turbine system are provided in the table below.

Table 1. Specifications of the DFIG Generator

DFIG Characteristics	Value
Number of poles	4
Generator speed	900-2100 rpm
Mutual inductance Lm	3.0 p.u.
Stator leakage reactance Ls	0.10 p.u.
Rotor leakage reactance Lr	0.08 p.u.
Stator resistance Rs	0.01 p.u.
Rotor resistance Rr	0.01 p.u.

The stator currents related to the d and q components are shown in Figures 1 and 2. As observed, the rotor currents of all the wind turbines reach consensus and synchronize.

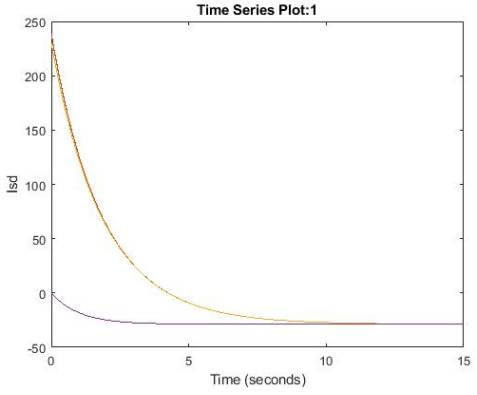

Fig. 1. The d component of the stator output currents.

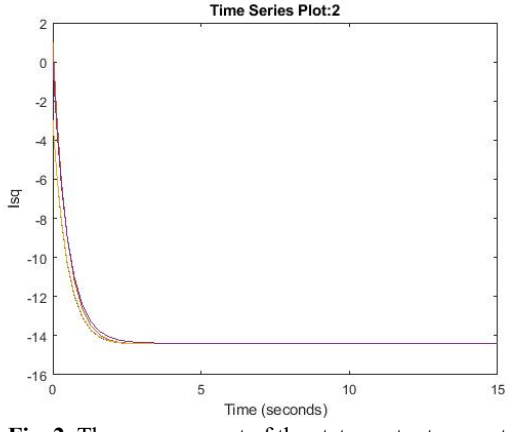

Fig. 2. The q component of the stator output currents.

The simulation results for the d and q components of the rotor currents are shown in Figures 3 and 4. As observed, the rotor currents of all the wind turbines converge and synchronize.

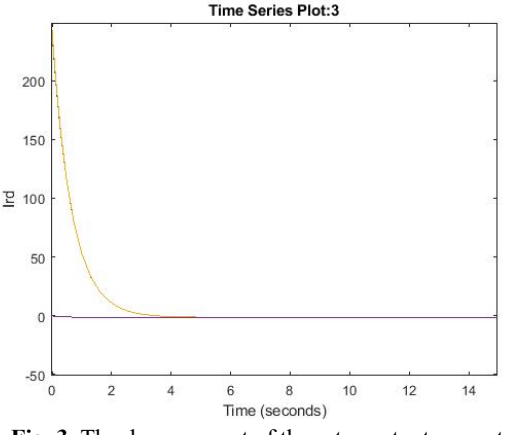

Fig. 3. The d component of the rotor output currents.

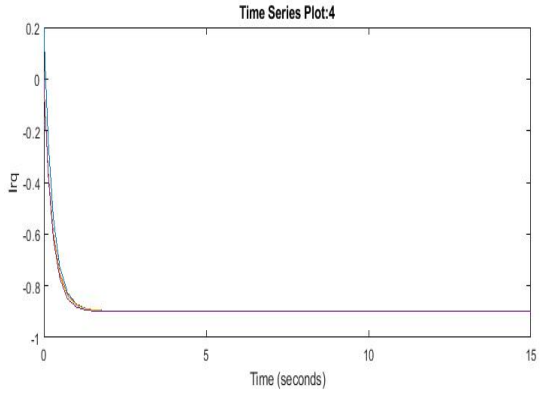

Fig. 4. The q component of the rotor output currents.

Additionally, the control inputs u_{eq}, u_r, and the overall control input u for each agent are presented below.

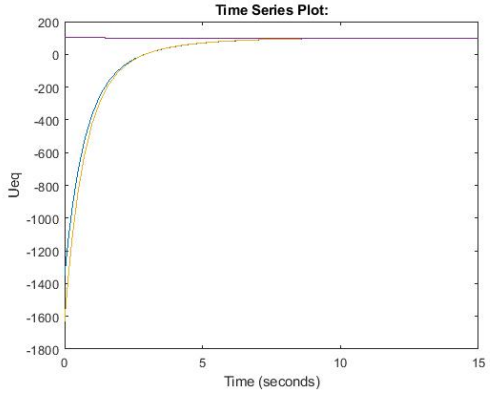

Fig. 5. The u_{eq} input for each agent.

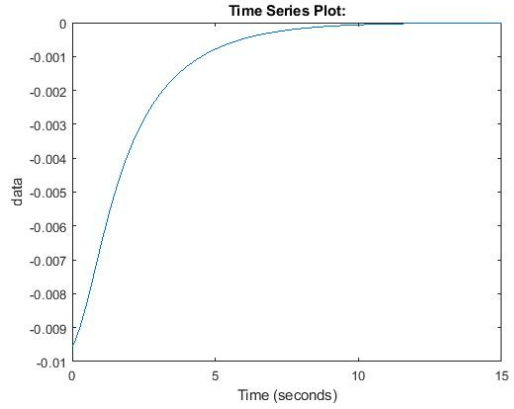

Fig. 6. The u_r input for each agent.

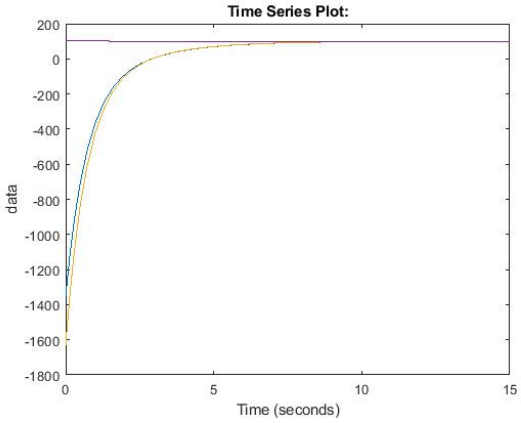

Fig. 7. The overall control input ufor each agent.

It is evident that consensus among the agents has been successfully achieved, and the follower agents accurately follow the leader agent. The controller demonstrates robustness against uncertainties and external disturbances.

4.2. Simulation and Results of the Designed Controller for Solar Cells

The simulation results for the d and q components of the output currents of the solar cell filters are shown in Figures 8 and 9. As observed, the output currents of all the solar cell filters converge and synchronize.

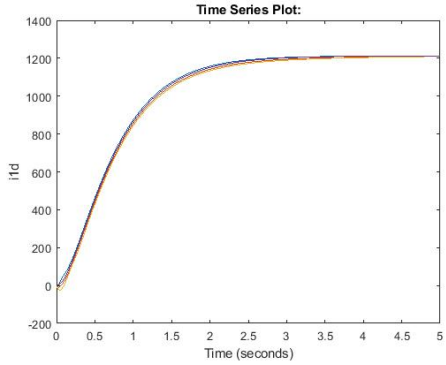

Fig. 8. The d component of the output currents of the solar cell filters.

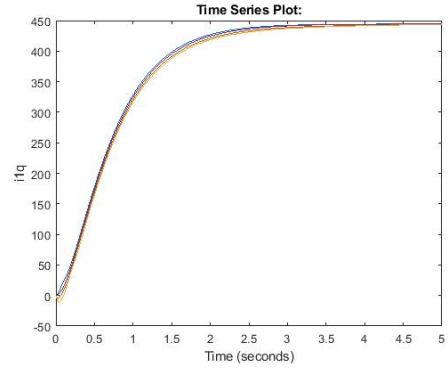

Fig. 9. The q component of the output currents of the solar cell filters.

The simulation results for the d and q components of the output currents of the solar cell inverters are shown in Figures 10 and 11. As observed, the output currents of all the solar cell inverters converge and synchronize.

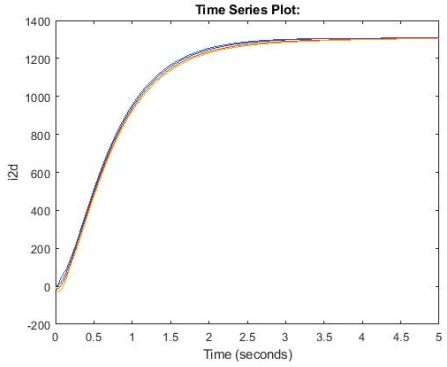

Fig. 10. The d component of the output currents of the solar cell inverters.

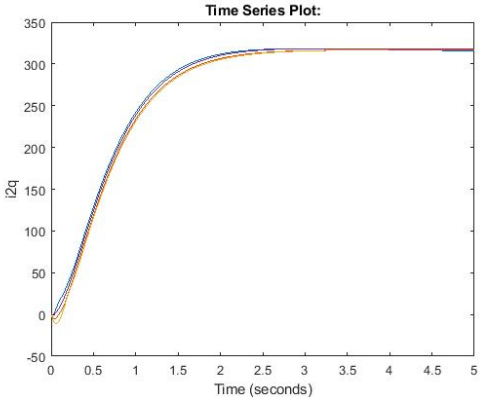

Fig. 11. The q component of the output currents of the solar cell inverters.

From the above figures, the following characteristics can be inferred:

1. Consensus among the agents and the corresponding leader is achieved.
2. The error between the state variables of the followers and the corresponding leader converges to zero.
3. The agents exhibit robustness in the presence of uncertainties.

5. CONCLUSION

In this paper, wind turbines and photovoltaic systems are considered as distributed generation agents, with each element treated as an individual agent. A multi-agent system is designed for these different agents to achieve consensus among them. The system is considered heterogeneous, which complicates the problem. To address this issue and transform the problem into a homogeneous one, it is assumed that identical agents have separate leaders. If all agents synchronize with each other, the heterogeneous problem effectively becomes solvable as a homogeneous problem.

The main advantages of the proposed method include:

1. Robustness against uncertainties.
2. Transformation of a heterogeneous problem into a homogeneous one using multiple leaders.
3. Overall system stability.
4. Synchronization among the agents.

Transparency Statement

The data supporting this study are available upon reasonable request to the corresponding author, subject to ethical and confidentiality considerations.

Acknowledgments

We would like to express our gratitude to all individuals who contributed to this project.

Declaration of Interest

The authors declare that they have no competing interests.

Funding

This research received no specific grant from any funding agency, commercial, or not-for-profit sectors.

REFERENCES

[1] Xiao, Q., & Huang, Z. K. (2016). Consensus of multi-agent system with distributed control on time scales. Applied Mathematics and Computation, 277, 54-71. https://doi.org/10.1016/j.amc.2015.12.028

[2] Zhao, L., Yu, J., Lin, C., & Yu, H. (2017). Distributed adaptive fixed-time consensus tracking for second-order multi-agent systems using modified terminal sliding mode. International Journal of Control. https://doi.org/10.1016/j.amc.2017.05.049

[3] Bidram, A., Lewis, F. L., Davoudi, A., & Ge, S. S. (2013). Adaptive and distributed control of nonlinear and heterogeneous multi-agent systems. 52nd IEEE Conference on Decision and Control. https://doi.org/10.1109/CDC.2013.6760875

[4] Bidram, A., Davoudi, A., Lewis, F. L., & Guerrero, J. M. (2013). Distributed cooperative secondary control of microgrids using feedback linearization. IEEE Transactions on Power Systems, 28 (3), 3462-3470. https://doi.org/10.1109/TPWRS.2013.2247071

[5] Lu, X., Lu, R., Chen, S., & Lü, J. (2013). Finite-time distributed tracking control for multi-agent systems with a virtual leader. IEEE Transactions on Circuits and Systems I: Regular Papers, 60 (2), 352-362. https://doi.org/10.1109/TCSI.2012.2215786

[6] Chen, H.-T., Song, S.-M., & Zhu, Z.-B. (2018). Robust finite-time attitude tracking control of rigid spacecraft under actuator saturation. International Journal of Control, Automation and Systems, 16 (X), 1-15. https://doi.org/10.1007/s12555-016-0768-1

[7] Liu, H., Cheng, L., Tan, M., & Hou, Z. (2014). Containment control of general linear multi-agent systems with multiple dynamic leaders: A fast sliding mode based approach. IEEE/CAA Journal of Automatica Sinica, 1 (2), 178-187. https://doi.org/10.1109/JAS.2014.7004542

[8] Wang, X., & Li, S. (2018). Finite-time consensus for disturbed multi-agent systems with unmeasured states via nonsingular terminal sliding-mode control. In Proceedings of the 11th International Conference on Intelligent Robotics and Applications (pp. 134-145). Springer International Publishing. https://doi.org/10.1007/978-3-319-62896-7_11

[9] Wang, X., & Li, S. (2016). Consensus disturbance rejection control for second-order multi-agent systems via nonsingular terminal sliding-mode control. In 2016 IEEE Conference on Control Applications (pp. 1037-1042). IEEE. https://doi.org/10.1109/CCA.2016.7587912

[10] Ren, C.-E., & Chen, C. L. P. (2015). Sliding mode leader-following consensus controllers for second-order non-linear multi-agent systems. IET Control Theory & Applications, 9 (11), 1692-1701. https://doi.org/10.1049/iet-cta.2014.0484

[11] Beainy, A., Maatouk, C., Moubayed, N., & Kaddah, F. (2016). Comparison of different types of generator for wind energy conversion system topologies. In 3rd International Conference on Renewable Energies for Developing Countries (REDEC) (pp. 1-6). IEEE. https://doi.org/10.1109/REDEC.2016.7577535

[12] Slootweg, J. G., Polinder, H., & Kling, W. L. (2001). Dynamic modelling of a wind turbine with doubly fed induction generator. In 2001 Power engineering society summer meeting. Conference proceedings (Cat. No. 01CH37262) (Vol. 1, pp. 644-649). IEEE.. https://doi.org/10.1109/PESS.2001.970114

[13] Bao, X., Zhuo, F., Tian, Y., & Tan, P. (2013). Simplified feedback linearization control of three-phase photovoltaic inverter with an LCL filter. IEEE Transactions on Power Electronics, 28 (6), 2739-2752. https://doi.org/10.1109/TPEL.2012.2225076

[14] Zehfuss, J. G. (1858). Ueber eine gewisse Determinante. Zeitschrift für Mathematik und Physik, 3, 298-301.

[15] Lewis, F. L., Zhang, H., Hengster-Movric, K., & Das, A. (2013). Cooperative control of multi-agent systems: Optimal and adaptive design approaches. Springer Science & Business Media. https://doi.org/10.1007/978-1-4471-5574-4